Available online at www.sciencedirect.com
SCIENCE DIRECT®
Acta Materialia 53 (2005) 449–454
Acta MATERIALIA
www.actamat-journals.com

Strain rate dependence of deformation mechanisms in a Ni–Ti–Cr shape-memory alloy

Sia Nemat-Nasser *, Jeom Yong Choi

Department of Mechanical and Aerospace Engineering, Center of Excellence for Advanced Materials, University of California, San Diego, 9500 Gilman Drive, La Jolla, CA 92093-0416, USA

Received 14 July 2004; accepted 1 October 2004
Available online 13 November 2004

Abstract

The compressive response of a Ni–Ti–Cr shape-memory alloy is investigated at various initial temperatures, over a wide range of strain rates, using an Instron hydraulic testing machine and one of the CEAM/UCSD's modified split Hopkinson bar systems. The alloy is superelastic over a range of initial temperatures and strain rates, for strains less than about 5%. The transition stress for the stress-induced martensite formation, the yield stress of the resulting martensites, and the yield stress of the parent austenite show strain-rate sensitivity, all increasing monotonically with the increasing strain rate. The transition stress is less than the yield stress of the parent austenite (which is less than the yield stress of the resulting martensite) over a wide range of strain rates, but it eventually exceeds this yield stress once a *critical* strain rate is exceeded. Inelastic deformation at strain rates below the critical level begins by stress-induced martensite formation and continues by subsequent plastic yielding of the martensites, whereas at strain rates above the critical, inelasticity directly stems from the dislocation-induced plastic deformation of the parent austenite with minimal (if any) austenite-to-martensite phase transformation. The strain rate significantly affects the superelastic and yielding behavior of this shape-memory alloy within the superelastic temperature range.

Keywords: Ni–Ti–Cr; Split Hopkinson bar; Superelasticity; Initial temperature; Yield stress; Critical strain rate

1. Introduction

Shape-memory alloys can sustain large deformations without a permanent residual strain. This is called *superelasticity*. It occurs over a range of temperature by reversible phase transformation from the austenite to the stress-induced martensite under the action of an applied stress [1]. This superelastic property may be used for energy absorption (e.g., seismic protection of structures [2–4]) or to develop actuators [5–7]. In many applications of this kind, the high strain-rate properties of the shape-memory alloys are of central importance.

Chen et al. [8] and Nemat-Nasser et al. [9,10] have studied the superelastic response of Ni–Ti alloys using a split Hopkinson bar technique. In particular, Nemat-Nasser et al. [10] report the existence of a critical strain rate, below which the material deforms by the formation of stress-induced martensites, whereas above this critical strain rate, the material deforms directly by dislocation-induced slip of the parent austenite even within the superelastic temperature and strain range.

In the present study, a ternary Ni–Ti–Cr alloy is heat-treated at 973 K for 60 min in order to decrease the overall stress level for the stress-induced martensite and also the yield stress of the resulting martensite. Then, the influence of the strain rate on the material's response is investigated at various initial temperatures in the range 296–373 K, using an Instron hydraulic testing

* Corresponding author. Tel.: +1 858 534 4914; fax: +1 858 534 2727.
E-mail address: sia@ucsd.edu (S. Nemat-Nasser).

1359-6454/$30.00
doi:10.1016/j.actamat.2004.10.001

machine and the CEAM/UCSD's split Hopkinson bar systems. In addition, the yield stress of the parent austenite is evaluated at an elevated temperature over a wide range of strain rates. Based on these experimental results, a deformation map is produced for this shape-memory alloy that shows the material's deformation characteristics in terms of the imposed strain rate.

2. Experimental procedure

A hot-rolled 52.62at.%Ni–47.09at.%Ti–0.29at.%Cr shape-memory alloy rod of 6.35 mm diameter is purchased from Special Metals Corporation. Circular cylindrical samples of 5mm nominal diameter and 5 mm nominal length are cut by electro-discharge machining (EDM). The specimens are annealed at 973 K for 60 min in air, followed by water quench to a temperature of 292 K. The transformation temperatures for the alloy are determined using a differential scanning calorimeter (DSC Q10); see Fig. 1. Measurements are carried out at temperatures from 120 to 320 K under a controlled heating/cooling rate of 10 K/min. The M_s and M_f are 257 and 235 K, and the A_s and A_f are 254 and 280 K, respectively.

Compression tests are performed over a range of strain rates from 10^{-3} to 10,000/s, at initial temperatures in the range of 296–373 K. The dynamic compression tests are carried out using CEAM/UCSD's recovery Hopkinson technique [11,12]. Fig. 2 is a schematic diagram of the split Hopkinson pressure bar, showing a striker bar, an incident bar, and a transmission bar. The specimen is sandwiched between the incident and transmission bars. Both ends of the specimen are greased to reduce the end-friction effect on the specimen deformation during the dynamic test. A furnace attached to the Hopkinson bar system is used to attain an elevated temperature [12]. Experimental techniques for shape-memory alloys are discussed in detail by Nemat-Nasser et al. [9,10]. Earlier work using Hopkinson bar techniques to study this class of alloys, includes [13–16].

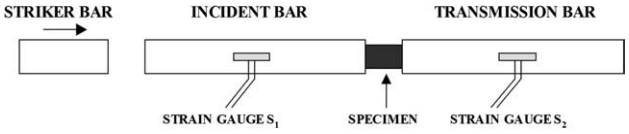

Fig. 2. Schematic diagram of the split Hopkinson bar.

Quasi-static compression tests are also performed using an Instron hydraulic testing machine. For elevated initial temperatures, a high-intensity quartz lamp is used to control the temperature to within ±2 K. The temperature is measured by a thermocouple, attached to the sample surface. The specimen deformation is measured by LVDT, mounted in the testing machine and calibrated before each test. To reduce the end friction, the sample ends are lightly polished and greased prior to each test.

3. Experimental results and discussion

3.1. Plastic response at 296 K initial temperature

Quasi-static and dynamic responses of a Ni–Ti–Cr alloy that is annealed at 973 K for 60 min, are investigated at 296 K initial temperature. Fig. 3 shows the time-variation of the strain in dynamic tests without pulse shaping [10]. The resulting strain rates vary in time in these experiments. For the 6 in. striker, the resulting strain rate in Fig. 3 can be divided into two sections,

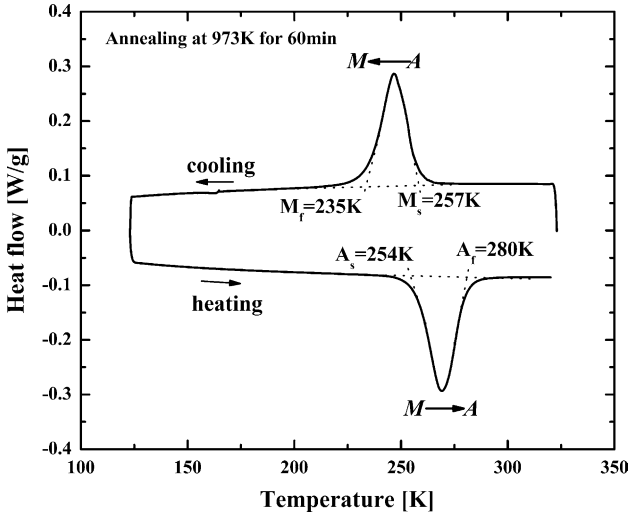

Fig. 1. DSC result of the sample annealed at 973 K for 60 min: *A*, austenite; *M*, martensite.

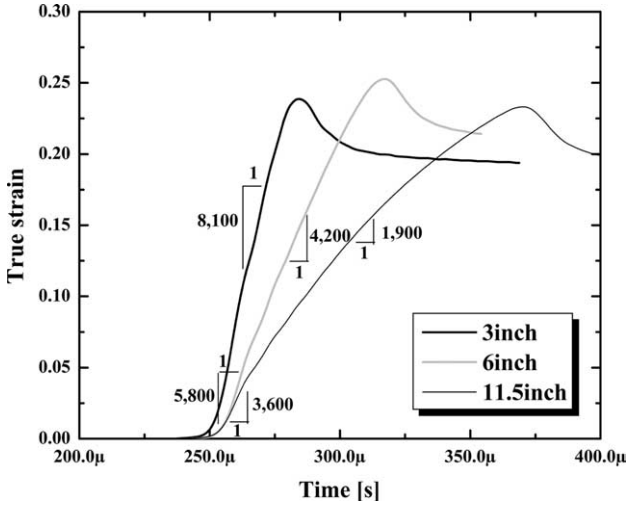

Fig. 3. Time-variation of strain in dynamic tests performed using a 1/2-in. Hopkinson bar system without pulse shaping.

based on the material response, i.e., a section corresponding to the superelastic response, and another section where the material has deformed by plastic slip. For the superelastic section, the strain is less than about 5%, whereas above this strain, plastic deformation takes place. In the case of a 3-in. striker bar, the strain varies linearly with time, indicating that deformation has occurred at a constant strain rate.

Fig. 4 exhibits the variation of the stress as a function of the strain at indicated strain rates in quasi-static and dynamic tests. The indicted strain rates for the dynamic tests are calculated for strains below 5%, thus corresponding to the superelastic deformation sections in Fig. 3. These results clearly show that the response of this material is strain-rate dependent. At strain rates below 5800/s (obtained with a 6-in. striker bar), the stress–strain curves correspond to the typical superelastic response of the shape-memory alloys. The transition stress is indicated by a solid triangle, marking the stress for the stress-induced martensite formation. The stress level denoted by a solid diamond, represents the yield stress of the resulting martensite. At an 8100/s strain rate, there is only one transition stress (indicated by an arrow on the stress–strain curve), and this corresponds to the yield stress of the parent austenite phase. As is seen, the transition stress for the stress-induced martensite formation increases with the increasing strain rate, and finally it disappears at strain rates beyond a critical level. For this annealed shape-memory alloy, the critical strain rate is between 5800 and 8100/s.

3.2. Yield stress of the parent austenite

To determine the yield stress of the parent austenite, quasi-static tests are carried out at a strain rate of 10^{-3}/s and various initial temperatures. Fig. 5 shows the effect of the initial temperature on the mechanical response of the material. At 296 K, the Ni–Ti–Cr alloy is superelastic for strains below 5%. Beyond this strain, plastic yielding of the resulting martensite is observed. Therefore, the stress–strain curve exhibits two transition stresses, as is mentioned before. At initial temperatures above 333 K, only one transition stress, which corresponds to the yield stress of the parent austenite, is observed. In this regime, the material in the austenite phase deforms by the dislocation-induced slip. The yield stress decreases as the initial temperature is increased above 333 K for the quasi-static deformation. A similar conclusion, however, cannot be obtained from the limited data shown in Fig. 6 for the dynamic case, although the flow–stress curve for 388 K initial temperature falls below that for the 333 K initial temperature. Fig. 7 displays the corresponding time-variation of the strain at indicated initial temperatures, obtained using a 1/2-in.

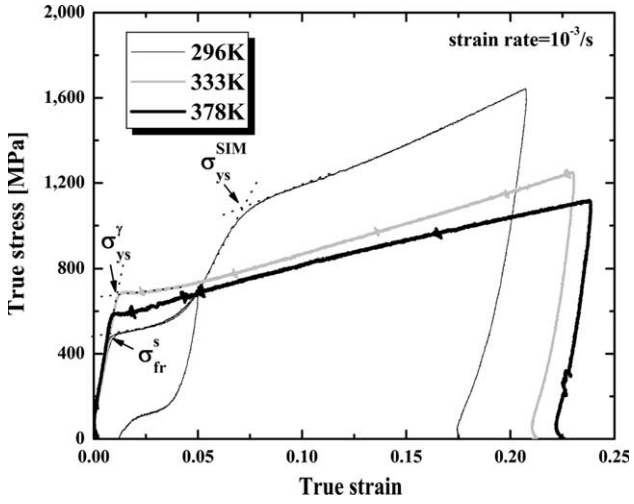

Fig. 5. Quasi-static variation of stress with strain for indicated initial temperatures.

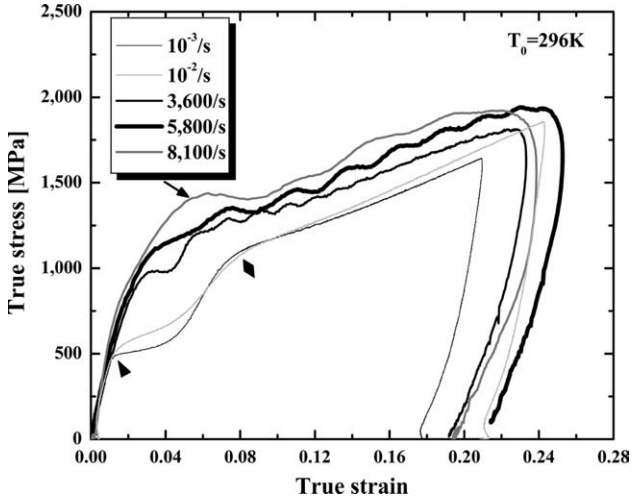

Fig. 4. Variation of stress with strain for indicated strain rates.

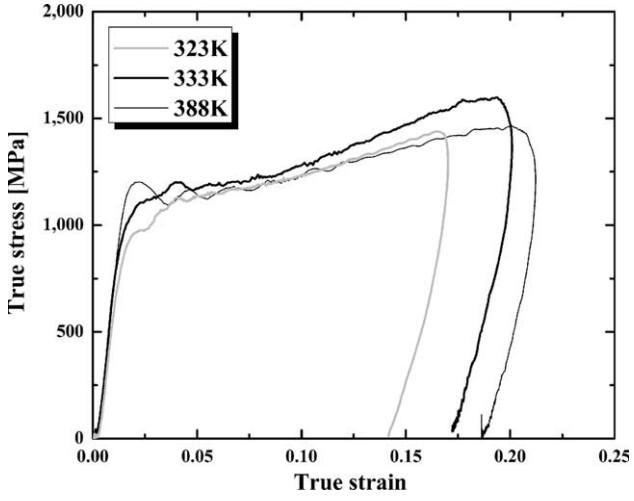

Fig. 6. Variation of stress with strain at indicated initial temperatures, obtained using a 1/2-in. Hopkinson bar without a pulse shaper.

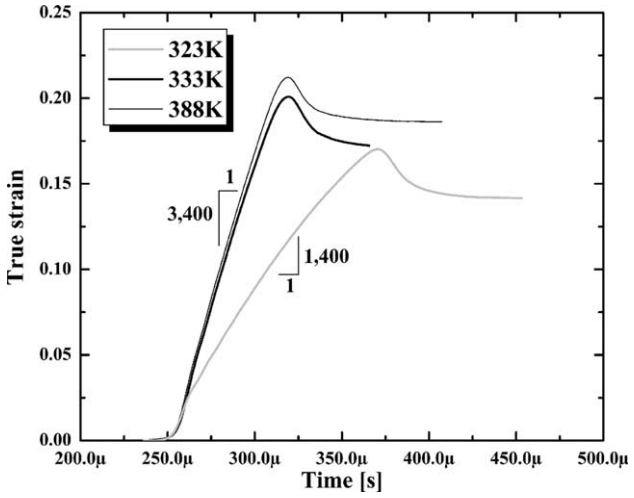

Fig. 7. Time-variation of strain at indicated temperatures, obtained using a 1/2-in. Hopkinson bar without a pulse shaper.

Hopkinson bar without a pulse shaper. A 6-in. striker bar is used for these tests. It is observed that the strain rate (slope) depends on the initial temperature. At temperatures above 333 K, the strain rate is almost constant. In addition, only one transition stress that corresponds to the yield stress of the parent austenite is displayed; see Fig. 6. However, at temperatures below 333 K, the strain rate (slope) is similar to that obtained in the superelastic temperature range. Based on the quasi-static and dynamic experimental results, it appears that the yield stress of the parent austenite can be directly measured at an approximately 333 K temperature.

3.3. Deformation mechanisms

Fig. 8 shows the variation with the strain rate of the stress for the stress-induced martensite formation and the yield stress of the resulting martensite. In addition, the yield stress of the parent austenite that is obtained at 333 K initial temperature, is included in Fig. 8. Here, the yielding of the parent austenite has occurred by the dislocation-induced slip, and thus the yield stress shows a strain-rate sensitivity similar to that observed in many other metals [17,18]. The yield stress for the dislocation-induced slip of the parent austenite phase is greater than the transition stress for the stress-induced martensite formation, ensuring a superelastic response for the material within its superelastic temperature range [19,20]. This superelasticity is observed at 296 K initial temperature. The yield stress at 333 K may be regarded as a minimum critical stress to produce dislocation-induced slip in the parent austenite at 296 K. As long as the transition stress for the stress-induced martensite formation is lower than the yield stress of the parent austenite, the shape-memory alloy deforms initially by the formation of the stress-induced martensites, also exhibiting superelasticity over a certain temperature range. As shown in Fig. 8, the transition stress and the yield stress of the parent austenite are strain-rate sensitive. They both increase gradually with the increasing strain rate until approximately 1000/s. Then, they both begin to increase rapidly as the strain rate increases above 1000/s. As suggested by Nemat-Nasser et al. [9,10], the strain-rate sensitivity of the transition stress may be explained by considering the interfacial motion of martensite phase, based on the thermal activation [21–23] and dislocation-drag models, similar to that of the dislocation-induced slip motion [18]. A similar dislocation-induced slip motion may also explain the yielding behavior of the parent austenite. The yield stress of the resulting martensite also increases monotonically with the increasing strain rate. As is shown in Fig. 8, both the transition stress and the yield stress of the parent austenite increase with the increasing strain rate, eventually crossing one another at a certain *critical* strain rate. At strain rates beyond this critical level, the transition stress for the stress-induced martensite is greater than the yield stress of the parent austenite.

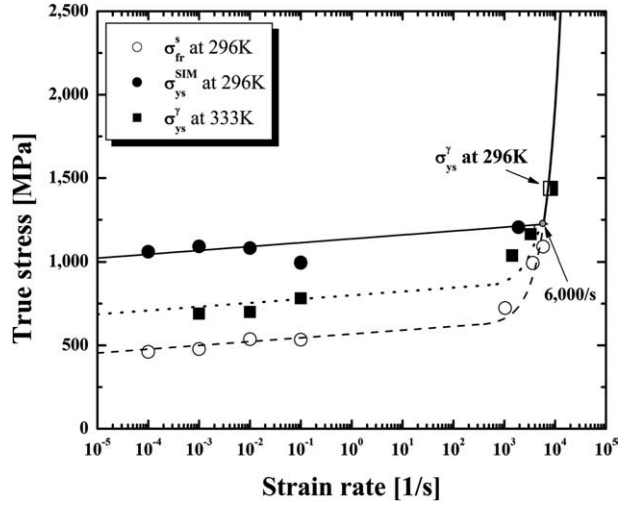

Fig. 8. The transition stress for the stress-induced martensite formation, the yield stress of the resulting martensite, and the yield stress of the parent austenite as functions of strain rate.

Within the superelastic temperature range, the stress-induced martensite formation and the dislocation-induced slip of the parent austenite are two competing mechanisms in the inelastic deformation of shape-memory alloys [19,20], with the mechanism that requires lower stress controlling the deformation mode. Therefore, at strain rates below the critical value, the shape-memory alloy tends to deform by the formation of the stress-induced martensite within the superelastic temperature range, resulting in a superelastic behavior. At strain rates beyond the critical value, the transition stress is greater than the plastic yield stress of the material. The deformation then occurs essentially by the dislocation-induced slip of the parent austenite, even if the temperature is kept within the superelastic range [10].

Fig. 9 shows the microstructure of this Ni–Ti–Cr alloy after it has been deformed at 296 K initial temperature beyond the superelastic strain range, at strain rates below (Fig. 9(a), 3600/s) and above (Fig. 9(b), 8100/s) the critical value. Below the critical strain rate, the material has deformed by the formation of stress-induced martensites. Above this strain rate, however, the material has deformed by the generation and motion of dislocations, as has also been reported by Nemat-Nasser et al. [10]. These authors observe a dislocation-induced cell microstructure at very high strain rates, above 10,000/s, but no strain-induced martensites with dislocation substructures that have been observed in shock impact tests by Thakur et al. [24].

Based on our experimental results, we now suggest a deformation map for this shape-memory alloy over a range of strain rates. The transition stress for the stress-induced martensite formation, the yield stress of the resulting stress-induced martensite, and the yield stress of the parent austenite are schematically given as functions of the strain rate in Fig. 10. As the strain rate is increased from quasi-static to dynamic levels, the martensite-formation stress, σ^{s}_{fr}, increases monotonically, eventually exceeding the yield stress of the parent austenite, σ^{γ}_{ys}, and the yield stress of the stress-induced martensites, σ^{SIM}_{ys} beyond a certain strain rate. The strain rate above which the martensite-formation stress exceeds σ^{γ}_{ys} is called *the critical strain rate*, and is denoted by $\dot{\varepsilon}_{cr}$. At strain rates below $\dot{\varepsilon}_{cr}$, the shape-memory alloy is superelastic under dynamic loading conditions. Its inelasticity is initially due to the formation of the stress-induced martensite, and then further loading produces the yielding of the resulting martensite by detwinning, reiorentation of the resulting stress-induced martenstie variants, and eventually by dislocation-induced slip deformation of the martensites. On the other hand, at strain rates above $\dot{\varepsilon}_{cr}$, the shape-memory alloy deforms inelastically directly by the dislocation-induced plastic slip of the parent austenite. At strain rates below $\dot{\varepsilon}_{cr}$, σ^{s}_{fr} increases gradually with the increasing strain rate up to about 1000/s, after which it increases dramatically as the strain rate is increased. In Fig. 10, we have suggested two potential mechanisms that may dominate the interfacial motion of the martensite phase at subcritical strain rates: (1) thermal activation at strain rates below about 1000/s, and (2) dislocation drag at higher strain rates. The yield stress of the *material* is marked by a thick solid line in this figure. At strain rates below the critical value, this yield stress represents the yielding of the resulting martensite, whereas at strain rates above this critical value, it represents the yielding of the parent austenite. The yield stress of the material increases gradually with the increasing strain rate, then it begins to increase rapidly with the increasing strain rate. Finally, above the critical strain rate, the yield stress increases with the increasing strain rate essentially due to the resistance to the motion of dislocations of the parent austenite.

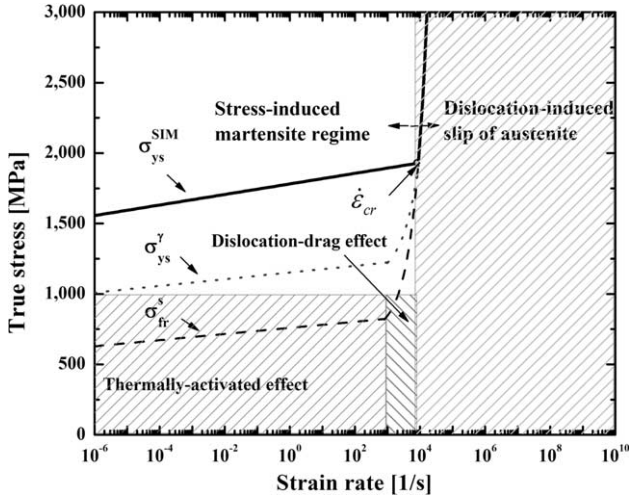

Fig. 10. Schematic deformation map of the shape-memory alloys as a function of strain rate.

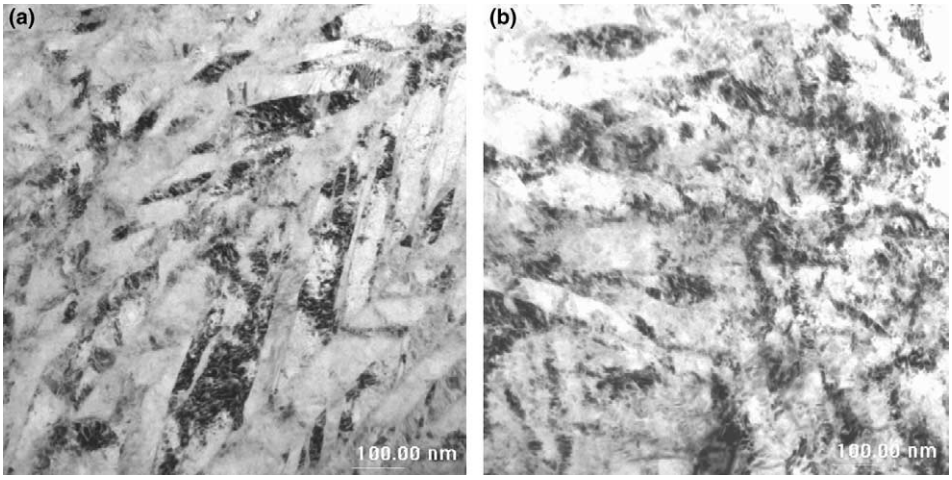

Fig. 9. TEM micrographs of Ni–Ti–Cr alloy that is deformed to strain beyond the superelastic range at 296 K initial temperature and at strain rates: (a) 3600/s and (b) 8100/s.

4. Summary and conclusions

Compressive tests are performed to investigate the deformation mechanism of a Ni–Ti–Cr shape-memory alloy, using an Instron hydraulic testing machine and one of the CEAM/UCSDs modified split Hopkinson bar systems. The Ni–Ti–Cr shape-memory alloy is heat-treated at 973 K for 60 min and then deformed at various strain rates. The experimental results show that the deformation of the shape-memory alloy is strongly strain-rate dependent. The rate sensitivity of the transition stress for the stress-induced martensite formation may be explained by the thermally-activated and dislocation-drag models. The transition stress and the yield stress of the parent austenite both increase with increasing strain rate and eventually attain a common value at a *critical* strain rate within the superelastic temperature range. At strain rates below the critical level, stress-induced martensites are formed, whereas the dislocation-induced slip deformation occurs at strain rates above this level. The yield stress of this material follows the yielding behavior of the resulting martensite at strain rates below the critical level, and the yield stress of the parent austenite for strain rates exceeding this level. It thus appears that the superelastic and yielding behaviors of shape-memory alloys are affected by both the temperature and the strain rate.

Acknowledgements

This work was supported by ONR (MURI) Grant N000140210666 to the University of California, San Diego. The authors express their appreciation to Mr. Jon Isaacs for his assistance in Hopkinson experiments.

References

[1] Otsuka K, Wayman CM, editors. Shape memory materials. Cambridge: Cambridge University Press; 1998.
[2] Tirelli D, Mascelloni S. J Phys 2000;IV10:665.
[3] Dolce M, Cardone D. Inter J Mech Sci 2001;43:2657.
[4] Saadat S, Salichs J, Noori M, Davood H, Bar-on I, Suzuki Y, et al. Smart Mater Struct 2002;11:218.
[5] Leo PH, Shield TW, Bruno OP. Acta Metall Mater 1993;41:2477.
[6] Tobushi H, Shimeno Y, Hachisuka T, Tanaka K. Mech Mater 1998;30:141.
[7] Millet JC, Bourne NK, Gray III GT. J Appl Phys 2002;92:3107.
[8] Chen WW, Wu Q, Kang JH, Winfree NA. Inter J Solids Struct 2001;38:8989.
[9] Nemat-Nasser S, Choi JY, Guo W-G, Isaacs JB, Taya M. J Eng Mater Technol 2004 [in press].
[10] Nemat-Nasser S, Choi JY, Guo W-G, Isaacs JB. Mech Mater 2004 [in press].
[11] Nemat-Nasser S, Isaacs JB, Starrett JE. Proc R Soc Lond A 1991;435:371.
[12] Nemat-Nasser S, Isaacs JB. Acta Mater 1997;45:907.
[13] Ogawa K. J De Phys 1988;C3:115.
[14] Ogawa K. J De Phys 1991;C3:215.
[15] Liu Y, Li Y, Ramesh KT. Philos Mag A 2002;82:2461.
[16] Liu Y, Li Y, Xie Z, Ramesh KT. Philos Mag Lett 2002;82:511.
[17] Johnson JN, Tonks DL. In: Schmidt SC, Dick RD, Forbes JW, Tasker DG, editors. Shock compression of condensed matter. Amsterdam: Elsevier Science Publishers; 1997. p. 371.
[18] Kapoor R, Nemat-Nasser S. Metall Mater Trans A 2000;31:815.
[19] Miyazaki S, Otsuka K. ISIJ Inter 1989;29:353.
[20] Liu Y, Galvin SP. Acta Mater 1997;45:4431.
[21] Grujicic M, Olson GB, Owen WS. J De Phys 1982;C4:173.
[22] Grujicic M, Olson GB, Owen WS. Metall Trans A 1985;16:1713.
[23] Grujicic M, Olson GB. Interf Sci 1998;6:155.
[24] Thakur AM, Thadhani NN, Schwarz RB. Metall Trans A 1997;28:1445.